CHEMPHYSCHEM

DOI: 10.1002/cphc.200800149

Pyrenyl Excimers Induced by the Crystallization of POSS Moieties: Spectroscopic Studies and Sensing Applications**

Hua Bai, Chun Li, and Gaoquan Shi*[a]

An ester (PBPOSS) of 1-pyrenebutyric acid (PBA) and 1-(2,3-propanediol)propoxy-3,5,7,9,11,13,15-isobutylpentacyclo-[9.5.1.1-(3,9).1(5,15).1(7,13)]octasiloxane (a polyhedral oligomeric silsesquioxane, POSS) is synthesized by simple one-step esterification. Thin films of PBPOSS fabricated by the spin-coating technique exhibit strong excimer emissions of visible light. Upon exposure to the vapours of nitroaromatic compounds, including trinitrotoluene and dinitrotoluene, the films show fast fluorescence quenching. The high performance of these gas sensors is due to the high excimer contents and good vapour permeability of the PBPOSS films. Spectroscopic studies indicate that the crystallization of the POSS moieties in PBPOSS films induce the formation of pyrenyl excimers.

1. Introduction

Pyrene-based compounds have been widely used as fluorescent probes in detecting nitroaromatic compounds, oxygen and biomolecules.[1–4] This is mainly because pyrene has a high quantum yield[5] and a strong affinity with analytes. However, the emission of pyrene is in the ultraviolet region (380 nm) and cannot be used for fabricating naked-eye sensors. One strategy for addressing this problem is to use the excimer emissions of pyrene derivatives at 450–500 nm.[6] There are many literature reports on fluorescent sensors based on pyrenyl excimers in solution, but this strategy seems unsuccessful in their thin fluorescent films.[7–9] To fabricate thin-film fluorescent sensors for gaseous analytes, spin-coating is one of the most convenient techniques for preparing the sensing layers. Unfortunately, the thin film of pyrene prepared by spin-coating shows only a weak excimer emission.[4] Although pyrene crystals emit a pure excimer fluorescence, spin-coated thin films of pyrene and its various derivatives exhibit weak or no excimer emissions.[10] This is mainly due to the rapid evaporation of solvent during the spin-coating process, which results in a random packing of pyrene rings. Furthermore, even if pyrene rings are forced to form excimers by tight aggregation, the analytes with large molecular sizes (e.g. trinitrotoluene, TNT) are difficult to diffuse into the film, which strongly slows down the response rate of the sensor.

The introduction of a functional substituent onto the pyrene ring may provide additional interactions for inducing the formation of pyrene excimers. For example, a monolayer film of 1-pyrenebutyric acid (PBA) shows strong excimer emission and has been applied for sensing oxygen.[3,10] In this case, the hydrogen bonding between carboxyl groups might play an important role in excimer formation. To increase the permeability of the sensing films, they have to be prepared as thin as possible or the pyrene rings grafted with bulky groups to prevent their tight aggregation. Recently, it was reported that a polyhedral oligomeric silsesquioxane (POSS) could effectively reduce the chain aggregations in the active layers of polymer light-emitting diode (PLED) devices.[11] Furthermore, POSSs crystallize easily in solid films,[12,13] which possibly provides a driving force for the formation of pyrene excimers. Herein, we report the synthesis of an ester (PBPOSS) of PBA and 1-(2,3-propanediol)propoxy-3,5,7,9,11,13,15-isobutylpentacyclo-[9.5.1.1(3,9).1(5,15).1(7,13)]octasiloxane (POSS) and its use as the sensing material for detecting nitroaromatic compounds. The spin-coated thin films of PBPOSS emit strong blue light at 475 nm because of the formation of a high content of pyrenyl excimers induced by the crystallization of POSS moieties. Nitroaromatic compound sensors based on quenching the excimer emissions of PBPOSS films exhibit fast and efficient responses.

2. Results and Discussion

2.1. UV/Vis and Fluorescence Spectra of PBPOSS

Figure 1 shows the UV/Vis spectra of a 2×10^{-6} M THF solution and a 9 nm film of PBPOSS. Both spectra show the characteristic absorbance bands of pyrene.[14,15] In the spectrum of the PBPOSS solution, the weak band at 374 nm is assigned to the weakly allowed $S_0 \rightarrow S_1$ transition. The other three bands at about 340, 270 and 240 nm are attributed to the transitions of S_0 to S_2 and higher states, respectively.[15] The absorbance bands in the spectrum of the PBPOSS film show a red shift of about 4 nm compared with those of the solution spectrum,

[a] H. Bai, Prof. C. Li, Prof. G. Shi
Department of Chemistry
Tsinghua University, Beijing 100084 (P. R. China)
Fax: (+86) 10-6277-1149
E-mail: gshi@tsinghua.edu.cn

[**] POSS: polyhedral oligomeric silsesquioxane

Supporting information for this article is available on the WWW under http://dx.doi.org/10.1002/cphc.200800149.

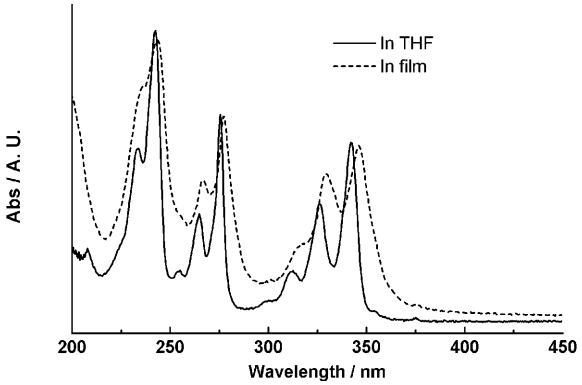

Figure 1. Normalized UV/Vis spectra of a 2×10^{-6} M THF solution and a 9 nm thick film of PBPOSS.

and their half-band widths are also slightly increased. This effect is mainly due to the changes in dispersion energy and static interaction energy between two pyrenyl groups as one or both are electronically excited.[16] The UV/Vis spectral results indicate that the pyrenyl groups are located close to each other in the PBPOSS film.

The excitation and emission spectra of a 2×10^{-6} M THF solution and a 9 nm film of PBPOSS are shown in Figure 2. Both the excitation and emission spectra of the PBPOSS solution are almost the same as those of pyrene.[17] The emission spectrum has two strong sharp bands at 378 and 398 nm (I and III bands) in addition to several shoulder bands.[5,18] No excimer emission band was observed in the spectrum of the dilute solution. In contrast, the emission spectrum of PBPOSS film shows weak emission bands of pyrene monomers, and exhibits a strong typical excimer emission at 475 nm.[6] The emission intensity ratio of the excimer band to the monomer band (I_{475}/I_{378}) was calculated to be about 26. The fluorescence quantum yields of PBPOSS were measured to be 0.39 in THF solution and 0.38 in film. Furthermore, there is a 4 nm red shift in the excitation spectrum of the film compared with that of the solution spectrum, which is also caused by the interaction between pyrene rings. Thus, it is reasonable to conclude that most pyrene rings in the PBPOSS film are aggregated into excimers.

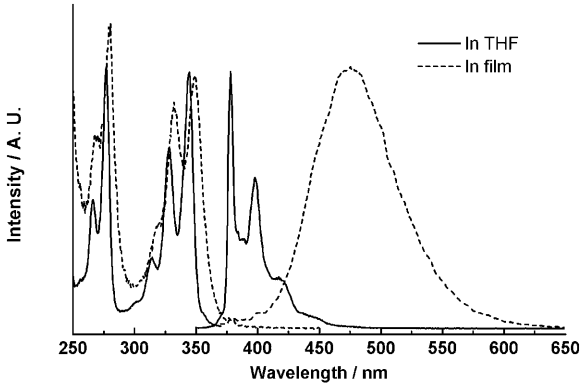

Figure 2. Normalized emission and excitation spectra of a 2×10^{-6} M THF solution and a 9 nm thick film of PBPOSS.

2.2. Fluorescence Quenching Studies

The spin-coated PBPOSS film showed rapid sensing of TNT vapour. Figure 3 presents the time-dependent fluorescence spectra of a 9 nm PBPOSS film upon exposure to TNT vapour. At room temperature, the fluorescence intensity of the film decreased by about 50% in 10 s and further to 93% in 60 s. These results indicate that this is one of the fastest TNT sensors

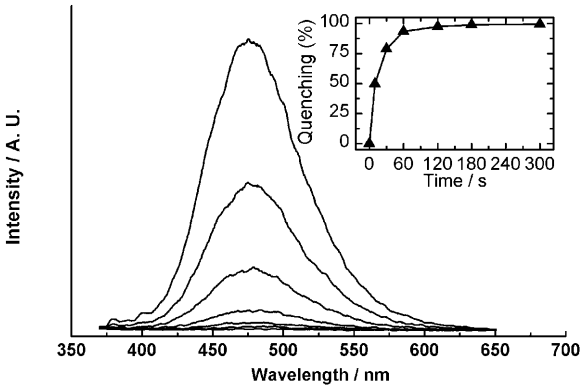

Figure 3. Fluorescence spectra of a 9 nm thick PBPOSS film upon exposure to TNT vapour for different times. From top to bottom, the exposure time was 0, 10, 30, 60, 120, 180 and 300 s, respectively. Inset: plot of quenching efficiency (%) versus time.

reported to date, and the response time is much shorter than that of sensors made from neat pyrene.[4] Moreover, the quenching process can be accelerated by reducing the thickness of the PBPOSS film. The fluorescence quenching curves of PBPOSS films with different thicknesses are shown in Figure 4. These films were prepared by spin-coating PBPOSS solutions with different concentrations of PBPOSS at the same spin rate. The overall features of the UV/Vis spectra are identical, which indicates that the molecular aggregation states in these films are the same (see Figure S1 in the Supporting Information). Therefore, the thicknesses of the films can be calculated from the absorbance of the films by referring to a known thickness value measured by an ellipsometer. As shown in Figure 4, the quenching efficiency decreases with the increase of film thickness, which indicates the reduction of TNT molecular permea-

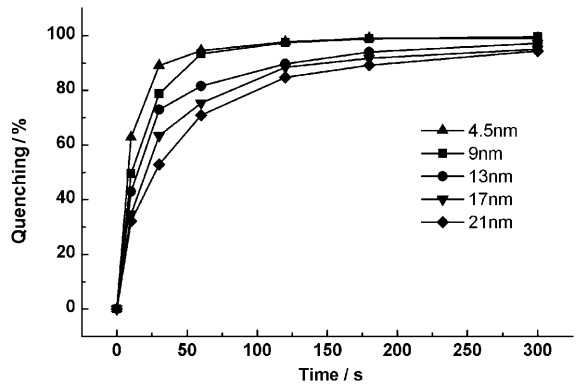

Figure 4. Time-dependent quenching efficiency of PBPOSS films with different thicknesses on exposure to TNT vapour.

bility in the film. The best sensing performance was exhibited by a 4.5 nm thick film, whose fluorescence intensity decreased by about 60% in 10 s. In contrast, for a 21 nm thick film, its fluorescence can be quenched by only 30% in 10 s and about 90% in 300 s. It is easy to understand the film thickness dependence of the quenching rate by considering the bulky size of the POSS group. In a 4.5 nm film, there are no more than four layers of PBPOSS molecules in the film, and thus TNT molecules can easily diffuse into the film and interact with the excited pyrenyl groups.

Fluorescence quenching of PBPOSS film towards 2,4-dinitrotoluene (2,4-DNT), nitrobenzene (NB) and nitromethane (NM) was also tested (Figures S6–S8). The quenching rate of a 9 nm PBPOSS film upon exposure to 2,4-DNT vapour is close to that of sensing TNT, while those of NB and NM are much slower. It is known that the electron transfer between probe and analyte molecules is controlled by its free energy change (ΔG), which can be calculated by Equation (1)[19,20]

$$\Delta G = E_{F/F^{+}\bullet} - \Delta E_{0-0} - E_{Q/Q^{-}\bullet} \quad (1)$$

where $E_{F/F^{+}\bullet}$ and ΔE_{0-0} are the redox potential and the lowest 0–0 excitation energy of the sensing element, respectively, and $E_{Q/Q^{-}\bullet}$ is the redox potential of the quencher. The $E_{Q/Q^{-}\bullet}$ values of 2,4-DNT (−1.0 V vs SCE) and NB (−1.15 V vs SCE) are both lower than that of TNT (−0.7 V). However, their vapour pressures are about 18 and 30000 times that of TNT, respectively. Thus, the low quenching rate of the 9 nm PBPOSS film upon exposure to NB vapour mainly results from the large free-energy change, and in the case of 2,4-DNT, the quenching rate is controlled by both vapour pressure and free-energy change. However, NM was found to have low quenching efficiency towards PBPOSS fluorescence, in spite of its high vapour pressure (4.5×10^{6} times that of TNT)[21] and high $E_{Q/Q^{-}\bullet}$ value (−0.84 V vs SCE).[22] This phenomenon implies that the molecular structure of the analyte also plays an important role in the quenching process.[4] Aromatic molecules are preferred to be absorbed in the PBPOSS film due to strong π–π interactions and their large, planar and unblocked LUMOs (π*) are also favourable to the electron-transfer process. That is why NM has a rather low quenching rate.

2.3. Mechanism Studies

To address the mechanism of the rapid fluorescence quenching of the PBPOSS film upon TNT exposure, a pure PBA film and a blend film of PBA and POSS were also prepared and studied for comparison. Figure 5 illustrates the UV/Vis and fluorescence spectra of a 2×10^{-6} M THF solution of PBPOSS and films of PBPOSS, PBA and PBA + POSS (1:1 molar ratio) with a thickness of 9 nm each. In comparison with those of the PBPOSS solution (Figure 5A), all the absorption bands of the films are red-shifted. The magnitude of the red shift ($\Delta\lambda$) for the $S_0\rightarrow S_2$ transition is in the sequence: PBA > PBA + POSS > PBPOSS. These spectral results implied that the interaction strength between pyrenyl groups in the films increased in the same trend. The interaction strength can be ascertained from

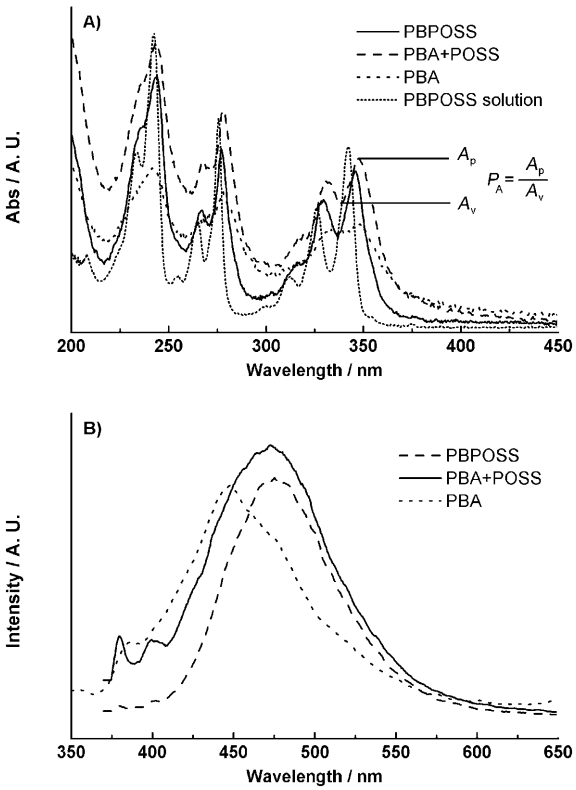

Figure 5. A) UV/Vis spectra of PBPOSS in THF solution (2×10^{-6} M) and of 9 nm thick films of PBPOSS, PBA + POSS (1:1 molar ratio) and PBA. B) Emission spectra of the three films. A_p: absorbance of the S_0-to-S_2 transition; A_v: absorbance at the adjacent valley.

the structural resolution of the UV/Vis spectra. As suggested by Herkstroeter et al.[23] and Winnik,[17] the loss in spectral resolution can be measured from the intensity ratio (P_A) of the absorption of the most intense band to that of the adjacent minimum at shorter wavelength. The larger the P_A value, the higher the spectral resolution. According to Figure 5A, the absorption spectrum of PBPOSS film with a P_A of 1.77 is the most structured, whereas the spectrum of PBA film has the lowest resolution ($P_A = 1.11$). This order is consistent with that that of $\Delta\lambda$, and also confirmed the trend of pyrene ring interaction strength described above.

The difference in pyrenyl aggregation in the films can also be confirmed by their fluorescence spectra (Figure 5B). All the films show strong excimer emissions, but the monomer emissions are still observable. In the spectra of PBA and PBA + POSS films, the monomer emissions are clearly stronger than that in the spectrum of PBPOSS film. This difference reflects the fact that the PBA and PBA + POSS films contain more pyrenyl groups in the monomer state than in PBPOSS. Furthermore, the emission maximum of PBA film (448 nm) is much shorter than that of PBPOSS film (475 nm), thus indicating an energy difference between the excimers in both films. The spectral results described above indicate that the introduction of the POSS moiety to PBA increased the excimer content of the film and also altered the excimer energy.

As described by Winnik,[17] there are two types of excimers: one is defined by Birks as the dimer associated in its electronic

excited state that is dissociated in its ground state;[6] the other is the so-called "static excimer", which is the dimer associated in both its electronic excited and ground states.[17] In a static excimer, the pyrenyl groups are close to each other, and exhibit perturbed absorption and excitation. Another characteristic of static excimers is that the excitation spectra monitored at the monomer and excimer emissions are different because of the energy-level difference of their ground states. The UV/Vis (Figure 5A) and excitation spectra (Figure 6) of the three films show broader vibronic bands, and the bands are also red-shifted in comparison with the corresponding bands of their dilute solutions, which indicates that the excimers are static ones. Furthermore, the excitation band monitored at the excimer emission shifts to a longer wavelength compared to that monitored at monomer emission, thus indicating the presence of ground-state interaction.

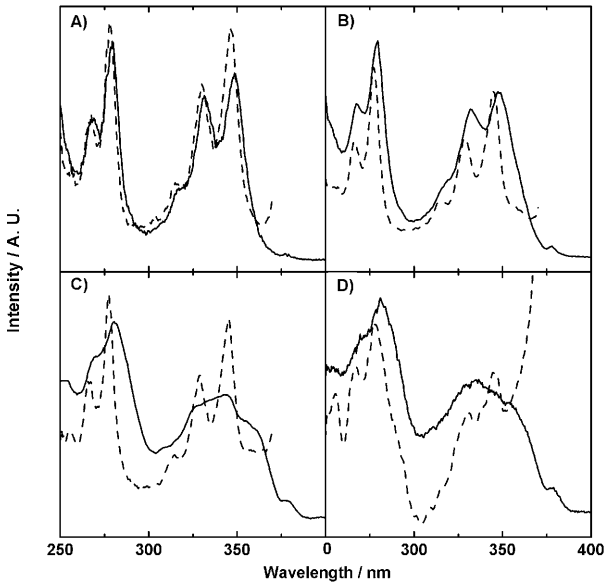

Figure 6. Excitation spectra of films of PBPOSS (A), PBA + POSS before (B) and after (C) exposure to TNT, and PBA (D) monitored at monomer emission (380 nm, -----) and excimer emission (474 nm, ——).

To study the excitation spectra quantitatively, the intensity ratio of the most intensive excitation band monitored at the emission band of the monomer or excimer to that of the corresponding valley at shorter wavelength is calculated and defined as P_M or P_E, respectively. (When measuring the emission intensity, the scattered light background was removed by subtracting an artificial linear baseline from 300 to 370 nm.) The P_M values of PBA, PBA + POSS and PBPOSS films are calculated to be 1.75, 2.66 and 2.57, respectively, while the corresponding P_E values are calculated to be 1 (without vibronic bands), 1.36 and 1.78. The trend of P_E values is reasonably the same as that of P_A. This fact further confirms that the interaction strengths of dimers in the films are in the order PBA > PBA + POSS > PBPOSS. Note that the excitation spectrum of the PBA + POSS film becomes less structured and its overall features are similar to those of PBA film after exposure in TNT vapour (Figures 6B and C).

The aggregation states of pyrenyl groups in the three films strongly influence their sensing performances. As shown in Figure 7, the PBA film, in which pyrene rings have the strongest interactions, exhibits poor sensing response to TNT vapour. In 10 s only 7% fluorescence was quenched, and the quenching efficiency reaches a saturated value of about 30% in 5 min. If PBA was mixed with an equal molar amount of

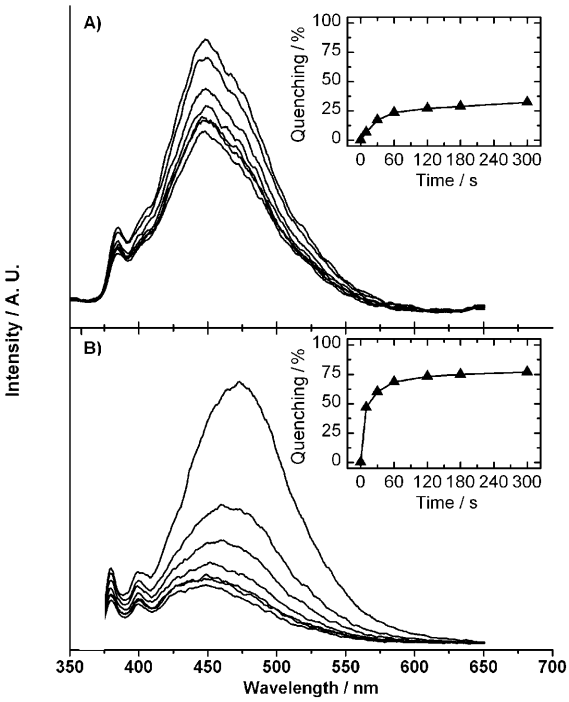

Figure 7. Fluorescence spectra of a 9 nm thick PBA film (A) and a PBA + POSS film (B) upon exposure to TNT vapour for different times. From top to bottom, the exposure times were 0, 10, 30, 60, 120, 180 and 300 s, respectively. Inset: plot of quenching efficiency (%) versus time.

POSS, the quenching efficiency of the spin-coated film was improved significantly. In the first 10 s, the fluorescence intensity decreased to 49% (see Figure 7B). However, successively the quenching rate decreased dramatically and also reached a saturated value of 80% in 5 min. Moreover, during the sensing process, the maximum of the excimer emission shifts from 474 to 448 nm. Finally, the blend film behaved like a PBA film. By combining the quenching rate sequence and the spectral facts described above, it is reasonable to conclude that strong pyrene interaction results in tight packing of the pyrene rings, which strongly reduces the contact probability between the analyte and sensing molecules.

The rapid response of the TNT sensor based on the PBPOSS film can be explained by its high excimer content and porous structure induced by bulky POSS moieties. The emission of the PBA film is consistent with that reported previously,[3,10] and also similar to those of the other pyrenyl-substituted carboxylic acids with longer alkyl chains. The strong interaction among pyrene rings in PBA film is mainly due to the hydrogen bonding of carboxyl groups, as confirmed by the red shift of the C=O stretching band in its infrared spectrum (Figure S9 in the

Supporting Information).[24] There is probably a cooperative effect of π–π interaction between pyrene rings and H bonding, thus leading to considerable aggregation of PBA molecules. It is difficult for TNT to diffuse into this compact film. As a result, the fluorescence quenching of the film upon TNT vapour exposure is ineffective. The excimers formed in this film emit light at 448 nm. The PBPOSS film has higher pyrenyl dimer content than the PBA film, and it does not have strong H-bonding interactions. The formation of pyrenyl dimers in the PBPOSS film is possibly induced by the crystallization of its POSS moieties.

The X-ray diffraction (XRD) patterns (Figure 8) of PBPOSS and PBA + POSS films each show a diffraction line at $2\theta = 8.1^\circ$ (10.9 Å), whereas it is absent in the pattern of PBA film. This line can also be found in the XRD patterns of PBPOSS powder (Figure S11) and polymer films containing POSS moieties, and its position reflects the size of POSS.[11,12] The POSS crystals bring two neighbouring pyrene rings close to each other; however, they prevent extensive aggregation (many pyrene rings stacking together) due to the large size of the POSS groups and limited chain length of the alkyl spacer.

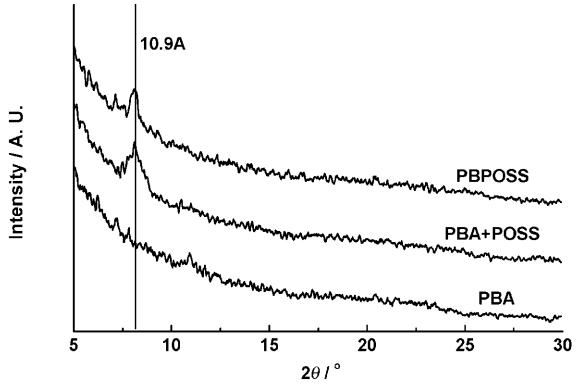

Figure 8. XRD patterns of PBPOSS, PBA + POSS and PBA films.

A simple predicted packing model of PBPOSS molecules is illustrated in Figure 9. This structure resulted in the formation of pyrenyl excimers with an emission at 475 nm. Moreover, the POSS moieties "prop up" the film into a porous structure, and TNT molecules can diffuse into the film easily, which results in a fast fluorescence quenching. In the PBA + POSS blend film, there are two types of excimers. In this film, pyrene rings are not grafted on POSS by covalent bonds. Therefore, some of the PBA molecules are possibly connected to POSS crystals through H bonding and they behave like PBPOSS molecules showing an excimer emission at 475 nm. However, the other PBA molecules are heavily aggregated because of their weak interactions with POSS molecules. During the TNT sensing process, the former type of PBA molecules contact easily with analyte molecules due to their porous structure, similar to that of PBPOSS, whereas the possibility of TNT molecules contacting the latter, tightly packed, pure PBA domains is low. As a result, the emission at 475 nm of the composite film is quickly quenched and then the apparent emission band of the film shifts to 448 nm, which is associated with the latter type of PBA molecules. This is also why the excitation spectrum of the composite film changes after exposure to TNT vapour (Figures 6B and C) and explains the existence of the saturated quenching efficiency for sensing TNT.

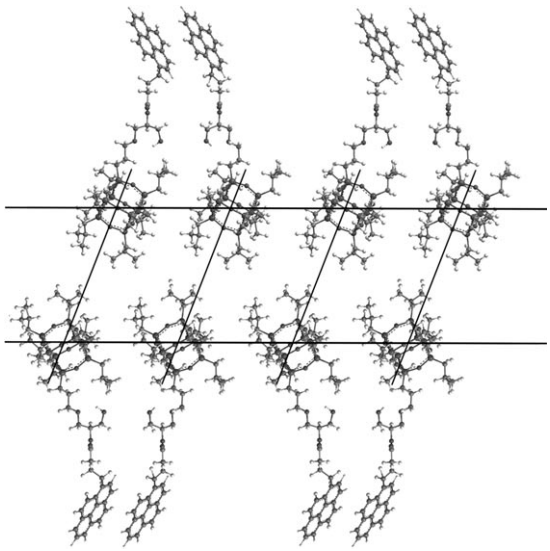

Figure 9. Predicted model of PBPOSS molecules in the film, which shows the crystallization of POSS and the formation of pyrene dimers.

3. Conclusions

We have successfully prepared fluorescent sensors based on thin PBPOSS films for the rapid detection of TNT. The films emit a blue light of pyrenyl excimers at 475 nm when excited at 350 nm. The fluorescence quenching of the sensor with a 4.5 nm PBPOSS film is as high as 60% after exposure to TNT vapour for 10 s at room temperature. To the best of our knowledge, this is one of the fastest thin-film sensors for TNT. A sensor based on PBA prepared under the same conditions exhibits a much slower and weaker fluorescence quenching. The crystallization of the POSS component makes two neighbouring pyrenyl groups in the ground state approach each other and induces the formation of a static excimer. In addition, the large POSS groups limit the number of aggregated pyrene rings in one unit, and generate a porous film. This accelerates the diffusion rate of analytes in the film. PBPOSS can be simply synthesized by a one-step reaction at room temperature, thus avoiding tedious organic synthesis, and the sensor can be fabricated conveniently by spin-coating. These factors make the thin-film TNT sensor based on PBPOSS more attractive for practical applications.

Experimental Section

Materials: PBA (97%), *N*,*N*′-dicyclohexylcarbodiimde (99%, DCC) and 4-dimethylaminopyridine (99%, DMAP) were purchased from Alfa Aesar Co., Ltd. POSS was bought from Aldrich Chemical Co. All the chemicals described above were used without further purification. Tetrahydrofuran (THF, Beijing Fine Chemical Co.) was purified by refluxing with sodium for several hours under nitrogen protection and then distilled to remove trace amounts of water.

Synthesis of PBPOSS: The procedure is depicted in Scheme 1. PBA (43 mg, 0.15 mmol), POSS (142 mg, 0.15 mmol), DCC (31 mg, 0.15 mmol) and DMAP (2 mg, 0.016 mmol) were dissolved in dichloromethane (20 mL) under stirring and then reacted at room temperature for 12 h. The reaction mixture was filtered to remove the white precipitate, then the filtrate was evaporated. Finally, the residue was purified by column chromatography (hexane/dichloromethane, 1:1) to give a light yellow powder. ^{1}H NMR (300 MHz, $CDCl_3$, Me_4Si): $\delta = 8.30$ (d, $J = 9.3$ Hz, 1H), 7.95–8.20 (m, 7H), 7.87 (d, $J = 7.9$ Hz, 1H), 5.18 (m, 1H), 3.82–3.57 (m, 4H), 3.41 (m, 4H), 2.51 (t, $J = 7.9$ Hz, 2H), 2.21 (m, 2H), 1.84 (m, 8H), 1.65 (m, 2H), 0.96 (d, 6.5 Hz, 42H), 0.60 ppm (d, $J = 7.2$ Hz, 14H); MALDI-TOF MS (*m/z*): 1237.7 $[M + H_2O + H^+]$, 1259.6 $[M + H_2O + Na^+]$ (Figure S11); elemental analysis calcd (%) for $C_{54}H_{90}O_{16}Si_8 \cdot H_2O$: C 52.39, H 7.49; found: C 52.16, H 7.50.

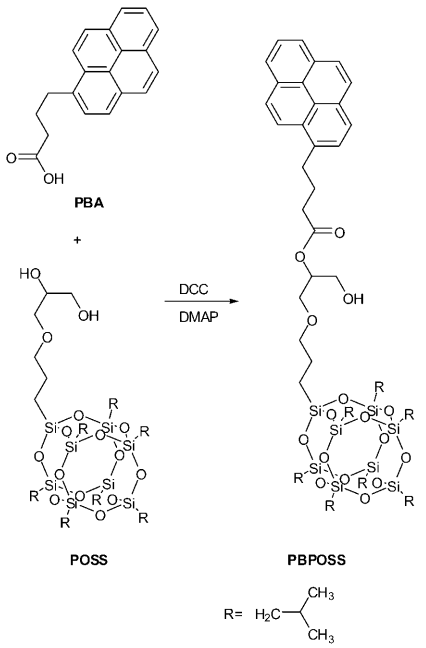

Scheme 1. Synthesis of PBPOSS.

Instruments and Characterization: All electrochemical experiments were carried out on a Model 273 potentiostat–galvanostat (EG&G Princeton Applied Research). The UV/Vis spectra were recorded on a U-3010 UV/Vis spectrometer (Hitachi). Fluorescence spectra were obtained with an LS 55 spectrometer (Perkin–Elmer). ^{1}H NMR spectroscopy was carried out on a JNM-ECA300 spectrometer (JOEL). MALDI-TOF mass spectrometry was carried out by using a BIFLEXIII mass spectrometer (Bruker). XRD patterns were collected on a Rigaku D/MAX 2500 diffractometer using $Cu_{K\alpha}$ radiation ($\lambda = 1.54056$ Å). The thickness of films was measured by the use of an ellipsometer Model GES5 (Sopra Corporation, France).

Fluorescence Quenching: PBPOSS, PBA and PBA + POSS films were prepared by spin-coating of their corresponding THF solutions ($0.1–2.5 \times 10^{-3}$ M) onto quartz substrates at a spin rate of 2400 rpm. The quartz substrate was cleaned by dipping in a mixture of H_2SO_4 and H_2O_2 (3:1 by volume; *caution: piranha solution is very corrosive and must be treated with extreme care; it reacts violently with organic materials*) for 2 h and then washing repeatedly with pure water. The as-prepared films were dried under vacuum at room temperature for 4 h before use. The quantum yields in THF and the film that were measured refer to pyrene in THF ($\phi_f = 0.79$)[5] and 9,10-diphenylanthracene in poly(methyl methacrylate) ($\approx 10^{-3}$ M, $\phi_f = 0.83$).[25]

The analyte (TNT, 2,4-DNT, NB or NM) was placed in a tiny vessel which was settled in a vial (40 mL) and kept at 28 °C for several hours to form saturated vapour. The fluorescence spectra of PBPOSS, PBA and PBA + POSS films were recorded immediately after each film was exposed to the analyte for a certain period. The quartz slice was placed in an ordinary fluorescence cell to make sure that for each measurement the sample was located in the same position. For all three films, the excitation wavelength was 350 nm.

Acknowledgements

This work was supported by the National Natural Science Foundation of China (20774056, 50533030, 20604013) and the 863 Project (2006AA03Z105).

Keywords: fluorescence · nitroaromatic compounds · pyrene · sensors · thin films

[1] W. Xu, R. Schmidt, M. Whaley, J. N. Demas, B. A. DeGraff, E. K. Karikari, B. A. Famer, *Anal. Chem.* **1995**, *67*, 3172–3180.
[2] S. J. Zhang, F. T. Lü, L. N. Gao, L. P. Ding, Y. Fang, *Langmuir* **2007**, *23*, 1584–1590.
[3] Y. Fujiwara, I. Okura, T. Miyashita, Y. Amao, *Anal. Chim. Acta* **2002**, *471*, 25–32.
[4] H. Bai, C. Li, G. Q. Shi, *Sens. Actuators B* **2008**, *130*, 777–782.
[5] D. S. Karpovich, G. J. Blanchard, *J. Phys. Chem.* **1995**, *99*, 3951–3958.
[6] J. B. Birks, *Rep. Prog. Phys.* **1975**, *38*, 903–974.
[7] S. K. Kim, J. H. Bok, R. A. Bartsch, J. Y. Lee, J. S. Kim, *Org. Lett.* **2005**, *7*, 4839–4842.
[8] B. N. Boden, K. J. Jardine, A. C. W. Leung, M. J. MacLachlan, *Org. Lett.* **2006**, *8*, 1855–1858.
[9] Y. Shiraishi, Y. Tokitoh, G. Nishimura, T. Hirai, *J. Phys. Chem. B* **2007**, *111*, 5090–5100.
[10] Y. Fujiwara, Y. Amao, *Sens. Actuators B* **2003**, *89*, 187–191.
[11] C. H. Chou, S. L. Hsu, S. W. Yeh, H. S. Wang, K. H. Wei, *Macromolecules* **2005**, *38*, 9117–9123.
[12] L. Zheng, A. J. Waddon, R. J. Farris, E. B. Coughlin, *Macromolecules* **2002**, *35*, 2375–2379.
[13] A. J. Waddon, E. B. Coughlin, *Chem. Mater.* **2003**, *15*, 4555–4561.
[14] R. S. Becker, I. Sen Singh, E. A. Jackson, *J. Chem. Phys.* **1963**, *38*, 2144–2171.
[15] Z. H. Khan, B. N. Khanna, *J. Chem. Phys.* **1973**, *59*, 3015–3019.
[16] R. V. Todesco, R. A. Basheer, P. V. Kamat, *Macromolecules* **1986**, *19*, 2390–2397.
[17] F. M. Winnik, *Chem. Rev.* **1993**, *93*, 587–614.
[18] P. C. Johnson, H. W. Offen, *J. Chem. Phys.* **1973**, *59*, 801–806.
[19] D. Rehm, A. Weller, *Ber. Bunsen-Ges.* **1969**, *73*, 834–849.
[20] M. Yanagidate, K. Takayama, M. Takeuchi, J. Nishimura, H. Shizuka, *J. Phys. Chem.* **1993**, *97*, 8881–8888.
[21] D. R. Lide, *Handbook of Chemistry and Physics*, CRC Press, Boca Raton, **1997**.
[22] M. S. Antelman, *The Encyclopedia of Chemical Electrode Potentials*, Plenum Press, New York, **1982**.
[23] W. G. Herkstroeter, P. A. Martic, S. E. Hartman, J. L. R. Williams, S. Farid, *J. Polym. Sci. Polym. Chem.* **1983**, *21*, 2473–2490.
[24] C. Li, B. Zhao, Y. Q. Lu, Y. Q. Liang, *J. Colloid Interface Sci.* **2001**, *235*, 59–65.
[25] J. S. Yang, T. M. Swager, *J. Am. Chem. Soc.* **1998**, *120*, 11864–11873.

Received: March 13, 2008
Revised: July 8, 2008
Published online on August 29, 2008

